Mutations in *KCND3* Cause Spinocerebellar Ataxia Type 22

Yi-Chung Lee, MD, PhD,[1,2,3] Alexandra Durr, MD, PhD,[4,5,6,7] Karen Majczenko, MD,[8,9] Yen-Hua Huang, MD, PhD,[10,11] Yu-Chao Liu, BS,[12] Cheng-Chang Lien, MD, PhD,[2,12] Pei-Chien Tsai, PhD,[2] Yaeko Ichikawa, MD, PhD,[13] Jun Goto, MD, PhD,[13] Marie-Lorraine Monin, MD,[4,5,6] Jun Z. Li, PhD,[14,15] Ming-Yi Chung, PhD,[16,17] Emeline Mundwiller, BS,[4,5,6] Vikram Shakkottai, MD, PhD,[9] Tze-Tze Liu, PhD,[18] Christelle Tesson, MS,[4,5,6,19] Yi-Chun Lu, BS,[3] Alexis Brice, MD,[4,5,6,7] Shoji Tsuji, MD, PhD,[13] Margit Burmeister, PhD,[8,14,15,20] Giovanni Stevanin, PhD,[4,5,6,7,19] and Bing-Wen Soong, MD, PhD[1,2,3,12]

Objective: To identify the causative gene in spinocerebellar ataxia (SCA) 22, an autosomal dominant cerebellar ataxia mapped to chromosome 1p21-q23.
Methods: We previously characterized a large Chinese family with progressive ataxia designated SCA22, which overlaps with the locus of SCA19. The disease locus in a French family and an Ashkenazi Jewish American family was also mapped to this region. Members from all 3 families were enrolled. Whole exome sequencing was performed to identify candidate mutations, which were narrowed by linkage analysis and confirmed by Sanger sequencing and cosegregation analyses. Mutational analyses were also performed in 105 Chinese and 55 Japanese families with cerebellar ataxia. Mutant gene products were examined in a heterologous expression system to address the changes in protein localization and electrophysiological functions.
Results: We identified heterozygous mutations in the voltage-gated potassium channel Kv4.3-encoding gene *KCND3*: an in-frame 3-nucleotide deletion c.679_681delTTC p.F227del in both the Chinese and French pedigrees, and a missense mutation c.1034G>T p.G345V in the Ashkenazi Jewish family. Direct sequencing of *KCND3* further identified 3 mutations, c.1034G>T p.G345V, c.1013T>C p.V338E, and c.1130C>T p.T377M, in 3 Japanese kindreds. Immunofluorescence analyses revealed that the mutant p.F227del Kv4.3 subunits were retained in the cytoplasm, consistent with the lack of A-type K^+ channel conductance in whole cell patch-clamp recordings.
Interpretation: Our data identify the cause of SCA19/22 in patients of diverse ethnic origins as mutations in *KCND3*. These findings further emphasize the important role of ion channels as key regulators of neuronal excitability in the pathogenesis of cerebellar degeneration.

ANN NEUROL 2012;72:859–869.

View this article online at wileyonlinelibrary.com. DOI: 10.1002/ana.23701

Received Mar 9, 2012, and in revised form Jul 12, 2012. Accepted for publication Jul 16, 2012.

Address correspondence to Dr Soong, Department of Neurology, National Yang-Ming University School of Medicine, Taipei Veterans General Hospital, #201, Sec 2, Shipai Road, Peitou District, Taipei, Taiwan 11217. E-mail: bwsoong@ym.edu.tw, bwsoong@gmail.com or Dr Stevanin, UPMC University Paris, Centre de Recherche du Cerveau et de la Moelle épinière, Hopital Pitie-Salpetriere, Paris, France. E-mail: giovanni.stevanin@upmc.fr or Dr Burmeister, Molecular and Behavioral Neuroscience Institute, University of Michigan, Ann Arbor, MI. E-mail: margit@umich.edu

From the [1]Department of Neurology, National Yang-Ming University School of Medicine, Taipei, Taiwan; [2]Brain Research Center, National Yang-Ming University, Taipei, Taiwan; [3]Department of Neurology, Taipei Veterans General Hospital, Taipei, Taiwan; [4]National Institute of Health and Medical Research, U975, Paris, France; [5]National Center for Scientific Research, UMR7225, Paris, France; [6]Pierre and Marie Curie University Paris, Brain and Spinal Cord Research Center, Pitie-Salpetriere Hospital, Paris, France; [7]Public Assistance Hospitals of Paris, Department of Genetics, Pitie-Salpetriere Hospital, Paris, France; [8]Molecular and Behavioral Neuroscience Institute, University of Michigan, Ann Arbor, MI; [9]Department of Neurology, University of Michigan, Ann Arbor, MI; [10]Department of Biochemistry, Faculty of Medicine, School of Medicine, National Yang-Ming University, Taipei, Taiwan; [11]Center for Systems and Synthetic Biology, National Yang-Ming University, Taipei, Taiwan; [12]Institute of Neuroscience, National Yang-Ming University, Taipei, Taiwan; [13]Department of Neurology, Graduate School of Medicine, The University of Tokyo, Tokyo, Japan; [14]Department of Human Genetics, University of Michigan, Ann Arbor, MI; [15]Department of Computational Medicine and Bioinformatics, University of Michigan, Ann Arbor, MI; [16]Faculty of Life Sciences and Institute of Genomic Sciences, National Yang-Ming University, Taipei, Taiwan; [17]Department of Medical Research and Education, Taipei Veterans General Hospital, Taipei, Taiwan; [18]Genome Research Center, National Yang-Ming University, Taipei, Taiwan; [19]Practical School of Advanced Studies, Paris, France and [20]Department of Psychiatry, University of Michigan, Ann Arbor, MI.

Additional Supporting Information can be found in the online version of this article.

Spinocerebellar ataxia (SCA) is a clinically, pathologically, and genetically heterogeneous group of dominantly inherited neurodegenerative disorders characterized by progressive cerebellar ataxia variably associated with pyramidal, extrapyramidal, bulbar, spinal, and peripheral nervous system involvement. Thirty-two dominant SCAs (labeled SCA1–36) have been chromosomally mapped, and the genes causing 20 of these disorders have so far been identified.[1,2] The genetic etiologies of many SCAs have yet to be elucidated.[3,4]

Previously, we characterized a large Chinese pedigree with an autosomal dominant ataxia spanning 4 generations.[5] The disease locus was mapped to chromosome 1p21-q23 and was designated SCA22.[5] The locus of SCA22 overlaps with that of SCA19 on 1p21-q21, previously identified in a Dutch family.[6,7] SCA19 and SCA22 were therefore proposed to be allelic with a worldwide distribution.[7] Here, we report mutations in *KCND3* in the original SCA22 family as well as in 5 other SCA families of French, Ashkenazi Jewish, and Japanese origin with dominant ataxia.

Subjects and Methods

Subjects

In family A of Han Chinese origin (Fig 1A), the original SCA22 family, we enrolled 31 members, including 13 affected, 6 unaffected, 6 at-risk, and 6 married-in individuals. The age at onset of ataxia in this pedigree ranged from 13 to 46 years. Clinical severity of ataxia was evaluated longitudinally using the 40-point (0 being normal) validated Scale for the Assessment and Rating of Ataxia (SARA).[8,9]

In family B, of French origin (see Fig 1B), including 8 affected individuals, 4 at-risk relatives, and 1 spouse participated in the study. Age at onset ranged from 24 to 51 years. Pathological nucleotide expansions were excluded in SCA1, 2, Machado–Joseph disease/SCA3, 6, 7, 10, 12, 17, 31, 36 and ATXN1 genes, as were mutations in (SCA5, 11, 13, 14, 23, and 28 genes).

Family C, of Ashkenazi Jewish American origin (see Fig 1C), was ascertained through a proband (III-3) with ataxia with onset in her 50s. Samples from her and an affected relative were negative by commercial DNA testing, excluding SCA1, 2, 3, 5, 6, 7, 8, 10, 13, 14, and 17 and DRPLA (Athena Diagnostics, Worcester, MA). Four affected and 3 unaffected subjects (including 1 apparently unaffected obligate carrier), along with 2 spouses participated in the study.

In addition, we screened for mutations in the candidate gene in DNA from the index patients of 105 Chinese and 55 unrelated Japanese families with cerebellar ataxia, in whom mutations in SCA1, SCA2, Machado–Joseph disease/SCA3, SCA6, SCA7, SCA8, SCA12, SCA17, SCA31, and ATXN1 genes had been excluded.

Written informed consent was obtained from all subjects according to study protocols approved by the institutional review boards of Taipei Veterans General Hospital, the Paris-Necker Ethics Committee, University of Michigan, and University of Tokyo. Genomic DNA was isolated from peripheral blood leukocytes following a standard protocol.[10]

Genetic Studies

Linkage Analysis. (Linkage analysis in family A to 1p21-q23 has been previously reported.[5]) In families B and C, genome scans were performed using Illumina (San Diego, CA) LINKAGE_12 microarrays (6,090 single nucleotide polymorphism [SNP] markers). Genotypes were determined using Beadstudio (Illumina) and analyzed with MERLIN 1.0.[11]

In family B, linkage analysis was run under a 0.85 penetrance model with equal allele frequencies, similar recombination fractions between males and females, and a disease frequency of 0.0005.

In family C, linkage analysis (run with 0.85 penetrance due to the presence of an unaffected obligate carrier female in the pedigree) identified ~200Mb regions on 8 different chromosomes with LOD scores between 0 and 2.0, reaching maximal LOD score of 1.97 on chromosome 1. To further narrow the regions, DNA of the most distantly related affected subjects (IV-6 and IV-7; see Fig 1C) was hybridized to Illumina Human660W-Quad high-density SNP BeadChips. PLINK[12] was used to identify chromosomal regions with large (>1,000kb) shared haplotypes.

(EXOME SEQUENCING.) Exomes were captured and enriched using either the Agilent SureSelect Human All Exon 50Mb kit (Agilent Technologies, Santa Clara, CA; families A and B) or the Nimblegen SeqCap EZ v1 (Roche, Indianapolis, IN; family C). The enriched samples were sequenced on the Illumina HiSeq2000 (Illumina) platform.

In families A and C, 2 affected subjects were sequenced, whereas in family B, DNA from 1 affected subject (III-6), the married-in parent (II-7), and 1 unaffected control subject were sequenced (see Fig 1). Only variants in the linked region and shared by both affected subjects sequenced (families A and C) or absent from the 2 controls (family B) were considered. Variants present in dbSNP, the 1000 Genomes Project,[13] the exome variant server (http://evs.gs.washington.edu/EVS/), or previously sequenced individuals without SCA were excluded. Variants were further filtered for those predicted to be functionally damaging, that is, nonsynonymous and splice variants. The details of exome sequencing, variants filtering, and analyses are available in the Supporting information.

Molecular analyses of KCND3

Mutational analysis of exons and their flanking introns of *KCND3* was conducted by polymerase chain reaction followed by direct nucleotide sequence analysis as previously described.[14]

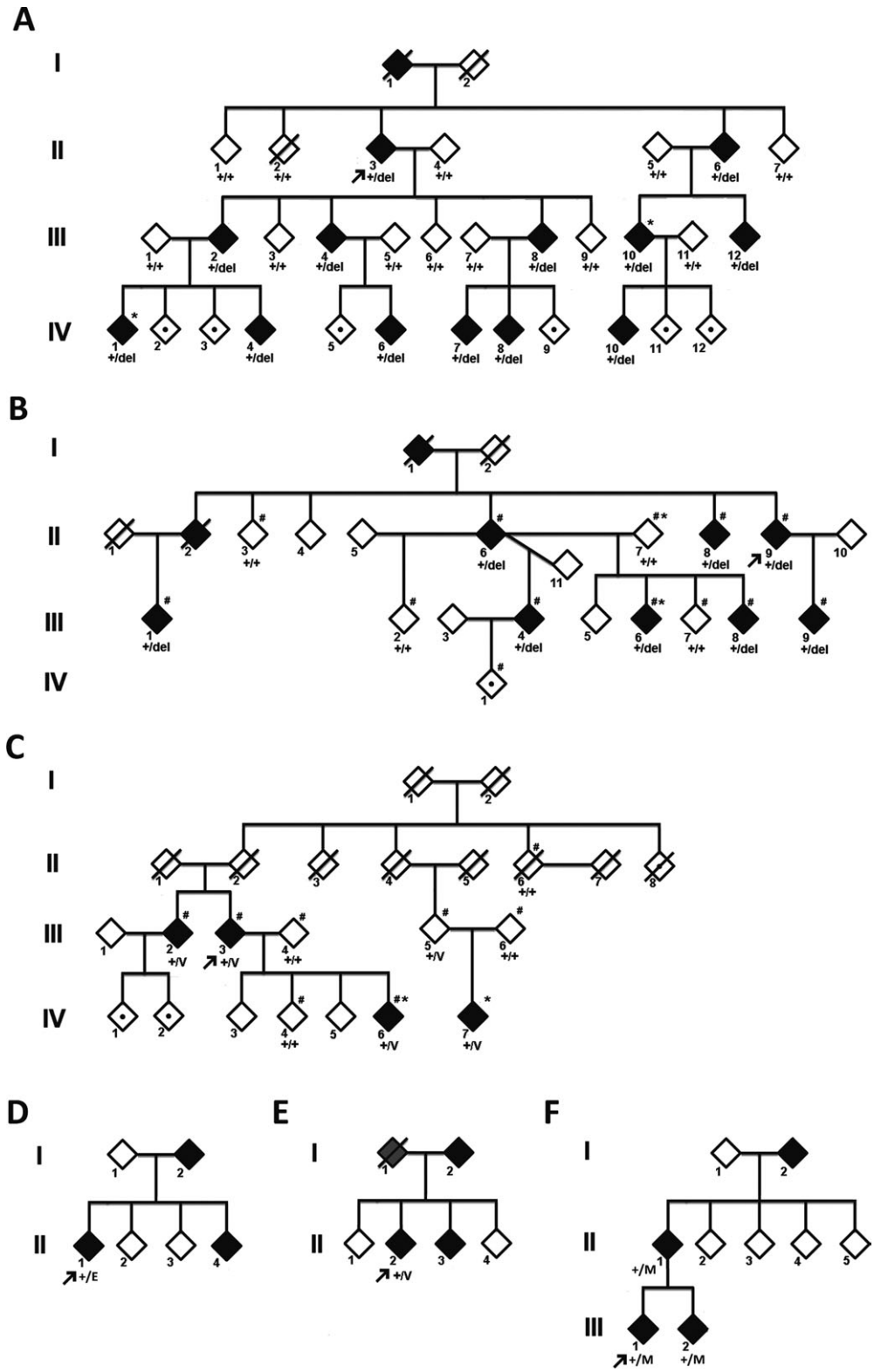

FIGURE 1: Pedigree charts of the families A, B, C, D, E, and F. The gender of the family members is obscured for privacy. The proband is denoted by an arrow. Filled diamonds represent affected members, grayed diamonds represent members with information suggesting but not confirming spinocerebellar ataxia, open diamonds indicate unaffected individuals, and those with a dot within an open diamond denote at-risk individuals. / = deceased; * = members who underwent whole exome sequencing; # = individuals included in linkage analysis; + = wild-type allele; del = allele with F227del; V = allele with G345V; E = allele with V338E; M = allele with T377M.

Expression Plasmids

A human Kv4.3 expression clone pE-11.GFPIre.hKv4.3L.WT was a generous gift of Dr J. M. Nerbonne (Washington University, St. Louis, MO).[15,16] The coding region of *KCND3* was subcloned into the pFLAG-CMV-5a vector (Sigma-Aldrich, St Louis, MO). The mutation c.679_681delTTC was introduced by site-directed mutagenesis using the Quick-Change method (Stratagene, Santa Clara, CA) and verified by bidirectional sequencing. The human Kv channel interacting protein 2 (KChIP2) expression clone was purchased from Open Biosystems (Thermo Scientific, Lafayette, CO). We constructed a plasmid expressing the integral membrane protein myelin protein zero (P0) fused to DsRed to mark the cell surface as previously described.[17] The endoplasmic reticulum (ER) markerp-DesRed-ER was purchased from Clontech (Mountain View, CA). All constructs were verified by sequencing.

Cell Culture and Transfection

Human embryonic kidney (HEK)-293T cells were maintained in high glucose Dulbecco modified Eagle medium supplemented with 10% fetal bovine serum (FBS) in a humidified incubator at 37°C under 5% CO_2. Cells were grown on glass coverslips in 6-well multiwell plates. Transient transfection was performed using the calcium phosphate precipitation method.[18] HEK293T cells were transiently transfected with plasmids (in 1:1:1 ratio, 200ng each) expressing Kv4.3 (either wild-type [WT] or the F227del mutant), KChIP2, and either P0-DsRed (to mark the cell surface) or DsRed-ER (to mark the ER).

Immunofluorescence Staining

Forty-eight hours after transfection, cells were fixed in 4% paraformaldehyde for 30 minutes, permeabilized with 0.2% Tween-20 for 30 minutes, and blocked with 1% bovine serum albumin for 30 minutes before incubation in primary antibody mouse anti-Kv4.3 at a dilution of 1:1,000 (ab99045; Abcam, Cambridge, UK) overnight at 4°C. Bound primary antibodies were detected using Alexa 488-conjugated goat antimouse immunoglobulin G (a11001; Invitrogen, Grand Island, NY).

Confocal Imaging

Images were captured with a Zeiss (Thornwood, NY) LSM 5 Pascal Laser Scanning Confocal system mounted on an Axiovert 200M inverted fluorescence microscope with a 63× oil immersion objective. Confocal imaging was performed on expression studies from 6 independent transfections. All images were processed and analyzed using ImageJ (National Institutes of Health, Bethesda, MD).

The midlevel optical section was selected for quantification of the surface expression of Kv4.3, with P0 staining to define the plasma membrane. A blank region was selected to calculate the average pixel intensity as the background, which was subtracted from all images. In the channel of the cell surface marker P0 signal, 20% of the maximum pixel intensity was set as the threshold to define the cell contour. Surface expression of Kv4.3 was calculated as the amount of Kv4.3 signal in the plasma membrane region normalized by the total signal intensity inside the cell contour.

Electrophysiological Recordings

HEK-293T cells were transfected with either WT or p.F227del Kv4.3 cloned into a Green fluorescence protein plasmid (pGFP) Ire vector, together with KChIP2 in a 1:1 ratio. Cells transfected with the vectors alone plus KChIP2 were used as controls. GFP-positive HEK-293T cells were used for electrophysiological recordings 48 hours after transfection. HEK cells were transferred to bath solution containing (in millimolars) NaCl 150, KCl 5, $MgCl_2$ 1, $CaCl_2$ 2.2, N-2-hydroxyethylpiperazine-N′-2-ethanesulfonic acid (HEPES) 10, and glucose 5; pH was adjusted to 7.3 with HCl. Transfected cells were visually selected by green fluorescence expression for recording under bright-field optics (BX51WI; Olympus, Tokyo, Japan). Patch pipettes (2–5MΩ) were pulled from borosilicate glass capillaries (outer diameter, 1.5mm; inner diameter, 0.86mm; Harvard Apparatus, Holliston, MA), heat-polished, and then filled with internal solution containing (in millimolars) K-gluconate 120, KCl 24, ethyleneglycoltetraacetic acid 0.2, and HEPES 10; pH was adjusted to 7.3 with KOH. Using a Multiclamp 700B amplifier (Molecular Devices, Union City, CA), whole cell patch recordings were made at 22 to 24°C. Pipette capacitance was compensated in cell-attached configuration, and patched cells were held in the voltage-clamp configuration at −90mV with series resistance (R_S) compensation (∼80–90%, lag, ∼0.5 milliseconds; R_S before compensation, 10–25MΩ). Potassium currents were evoked by voltage pulses (−80 to +70mV, 500 milliseconds; 10mV increments). Leakage and capacitive currents were subtracted using a P over −4 procedure. Membrane capacitances were determined from readout values (6–60pF) of membrane capacitance compensation on the patch amplifier. Potassium equilibrium potential (−86mV) was determined by the Nernst equation. Signals were low-pass filtered at 4kHz (4-pole Bessel) and sampled at 10kHz using the Digidata 1440 interface (Molecular Devices). Data acquisition was performed using the pClamp 10.2 software (Molecular Devices).

Results

Linkage Identifies SCA19/22 on 1p21-q23 as a Common Dominant Ataxia Locus

Families B and C with dominant adult onset ataxia were ascertained in France and in the USA in efforts to identify novel ataxia loci. Genome-wide low-density SNP chips followed by linkage analysis were used to identify candidate chromosomal regions. In family B, putative or uninformative linkage to 11 candidate regions was considered, including 6 regions reaching the maximal expected value of LOD score of 2.8 according to the pedigree structure (chromosomes 1, 2, 8, 9, and 14). In family C, high-density SNP chips and PLINK were used to identify shared haplotypes between the most distant relatives. Only 2 large shared haplotypes matched the linkage peaks, a 62Mb-long haplotype on chromosome 1 and a 33Mb haplotype on chromosome 15. The shared

haplotype with the highest LOD score on chromosome 1 overlapped the SCA22 region.

Exome Sequencing Identifies KCND3 Mutations in Families with Dominant Ataxia

In family A, after analysis and filtering, 11 heterozygous coding variants that mapped to 1p21-q23 were shared by both affected subjects and were not present in thousands of control samples in various databases (Supplementary Table 1). Sanger sequencing of these variants in the remaining 23 family members identified only 1 variant, c.679_681delTTC in *KCND3*, that completely segregated with the disease phenotype (Fig 2A). This mutation was not found in 500 normal Taiwanese-Chinese controls.

In family B, of 1,648 nucleotide variants present in the affected subject but absent in her married-in parent and the control, only 3 variants were heterozygous, absent, or rare in the Exome Variant Server and predicted to be damaging (Supplementary Table 2). Among these variants, c.679_681delTTC p.F227del in *KCND3* (see Fig 2B) was the strongest candidate, because mutations in the 2 other genes were known to have non-neurological phenotypes (detailed in the Supporting Information). This mutation cosegregated with the disease in the family and was absent from 152 French control chromosomes and in public database.

In family C, exome sequencing identified a large number of shared variants between the 2 affected individuals. After filtering by linkage and shared haplotypes, variants and that were predicted to be damaging, only 1 passed all filters, c.1304G>T p.G345V in *KCND3* (see Fig 2C; Supplementary Table 3). Conventional sequencing confirmed segregation in the family.

Mutation Screening in Chinese and Japanese Families with Hereditary Spinocerebellar Ataxias

No mutation in *KCND3* was found from any index patient of 105 Chinese families with hereditary ataxia.

Three missense mutations in *KCND3* were identified in 3 families among 55 Japanese families with ataxia (see Fig 1D): c.1013T>C p.V338E in exon 1 was found in family D, c.1034G>T p.G345V in exon 1 in family E, and c.1130C>T p.T377M in exon 2 in family F. None of these mutations was present in 96 Japanese controls or public databases.

SCA22-Associated Mutations Alter Highly Conserved Amino Acid Residues

All of the ataxia-associated mutations affect amino acids in Kv4.3 that are highly conserved across a wide variety of species, from zebrafish, frog, platypus, and mouse to humans (see Fig 2E). In silico analysis predicted deleterious consequences from the residue changes (Supplementary 4).

Clinical Features of Patients with KCND3 Mutations

Characteristically, the patients in the families with SCA19/22 all have a very slowly progressive cerebellar ataxia. In family A (Supplementary Table 5), II-3 has had difficulty walking for 35 years, with an onset at 46 years, and still manages to ride a 3-wheel motorcycle. III-2, at the age of 57 years (25 years after the onset of disease), has had a very slow progression of ataxia, with an average deterioration of only 0.3 SARA score point per year over the past 5 years. III-8 has been mildly ataxic for 31 years and yet only has a SARA score of 9 points at the age of 48 years. There has been no cognitive impairment, myoclonus, tremors, focal weakness, sensory loss, cogwheel rigidity, visual impairment, retinopathy, or ophthalmoplegia in any of the affected members. Brain magnetic resonance imaging (MRI) featured mild cerebellar atrophy (Supplementary Fig, A). Their electrocardiograms showed sinus rhythm with normal QT intervals. There was no arrhythmia on the 24-hour Holter monitor recordings. The echocardiograms were also unremarkable.

In family B (Supplementary Table 6), age at onset ranged between 24 and 51 years, and most patients have been seen at least twice to evaluate disease evolution. Progression was slow, as reflected by only 1 wheelchair user after 43 years of disease duration. Cerebellar ataxia was associated with impaired vibration sense at the ankles (3 of 8), with upward ophthalmoplegia (1 of 8) or with diplopia (1 of 8). Hyper-reflexes without positive Babinski sign was present in 3 of 8. Mild cogwheel rigidity was noticed in 2 patients at ages 61 and 77 years. In the absence of pyramidal involvement, urinary urgency/incontinence was seen in 5 of 8. Cerebellar atrophy was present in 5 patients with cerebral MRI (Supplementary Fig, B). The index case had sensory neuropathy.

In family C, the proband (III-3) is tripping and falling slightly more frequently now (once or twice each month), 10 years after the beginning of imbalance and slurred speech at the age of 55 years, which have only slightly progressed in the absence of any visual problem or dysphagia. Neurological examination revealed breakdown of the smooth pursuit with saccades, mild dysarthria, difficulty with heel-to-shin test, mildly wide-based gait, and difficulty with tandem walk. One of the 4 children, 1 of the siblings, and 1 of the first cousins also have had imbalance (Supplementary Table 7). Brain MRI revealed cerebellar vermian atrophy.

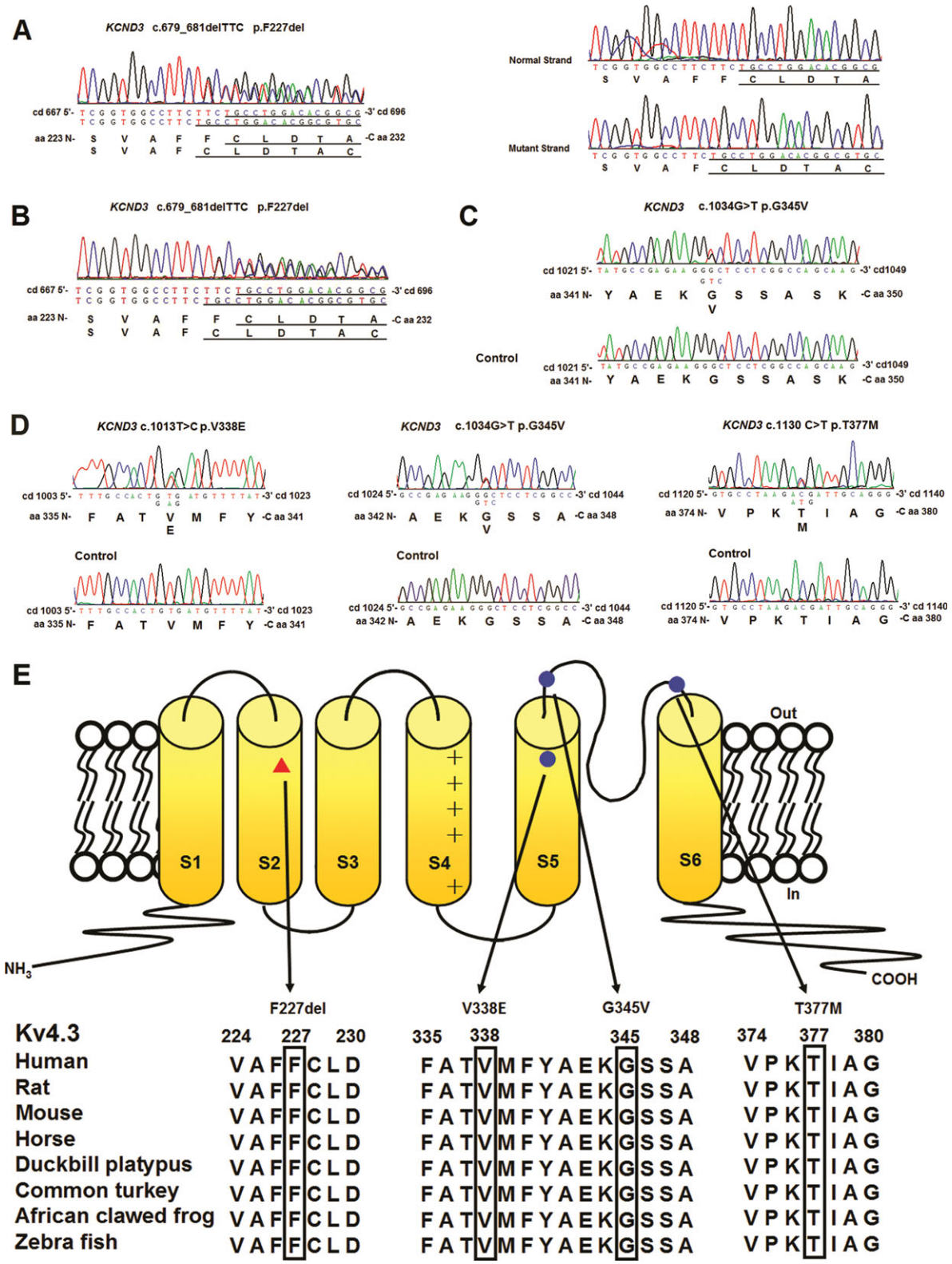

FIGURE 2: *KCND3* mutations and Kv4.3 membrane topology. (A–D) The electropherograms of *KCND3* heterozygous mutations. (E) Predicted Kv4.3 topology and locations of 4 mutations: red triangle, c.679_681delTTC (p.F227del); blue circles, c.1013T>C p.V338E, c.1034G>T p.G345V, and c.1130C>T p.T377M. The mutated residues are evolutionarily conserved, as shown by aligning protein sequences of Kv4.3 orthologs in various organisms.

In families D, E, and F, the age at onset was late, and the clinical progression of ataxia was also slow in the majority of the affected (Supplementary 8).

Immunofluorescence Studies

The immunofluorescence staining pattern of HEK-293T cells expressing either WT or p.F227del mutant Kv4.3 was characterized to address the question of channel protein localization. Cells expressing WT Kv4.3 displayed robust cell surface Kv4.3-specific staining, whereas virtually all cells expressing the mutant Kv4.3 demonstrated diffuse cytoplasmic Kv4.3-specific staining without discernible cell surface signal, suggesting impaired plasma membrane targeting of the mutant F227del Kv4.3 protein, which appeared to be abnormally retained in the cytoplasm and colocalized with an ER-specific marker (Fig 3). We observed no evidence of Kv4.3 in the mock-transfected cells. The expression of the cell surface marker P0 enabled us to define the cell membrane and quantify the subcellular localization of Kv4.3 using an unbiased approach. The ratio of cell surface expression for the p.F227del Kv4.3 was significantly lower than that observed in the WT Kv4.3 ($n = 10$; mean $\pm$ standard error of the mean, 0.28 ± 0.04 vs 0.61 ± 0.06; $p = 0.0014$).

Electrophysiological Recordings

In whole cell voltage-clamp recording on transfected HEK-293T cells, potassium currents were evoked by voltage pulses. In the control cells (KChIP2 + GFP), HEK-293T cells exhibited endogenous noninactivating outward currents (Fig 4). In contrast, large transient outward currents were observed in the WT Kv4.3-transfected HEK293T cells (WT Kv4.3 + KChIP2 + GFP). The outward currents recorded from p.F227del Kv4.3-transfected HEK293T cells (p.F227del + KChIP2 + GFP) were comparable to the endogenous potassium currents recorded from mock-transfected cells. After normalizing the current amplitude for cell size, WT Kv4.3-transfected cells had a significantly higher current density compared to p.F227del-transfected cells (WT: 0.52 ± 0.14 Nano-Ampere/pico-Faraday (nA/pF), $n = 8$; p.F227del: 0.09 ± 0.02 nA/pF, $n = 7$; $p < 0.0005$, Mann–Whitney test). The difference in current densities between p.F227del-transfected and control cells (p.F227del: 0.09 ± 0.02 nA/pF, $n = 17$; control: 0.09 ± 0.01 nA/pF, $n = 3$; $p = 0.67$, Mann–Whitney test) was not statistically significant. Given that the cell surface expression level of p.F227del Kv4.3 was minimal, the finding of low current densities by electrophysiological recordings is consistent with a notion of a defect in channel expression.

Discussions

Using exome sequencing and mutational analyses, we identified in 6 unrelated families of diverse ethnic origins with autosomal dominant cerebellar ataxia heterozygous mutations in the voltage-gated potassium channel Kv4.3-encoding *KCND3* gene. A 3-nucleotide in-frame deletion leading to p.F227del cosegregated with ataxia in family A of Han Chinese origin and family B of French origin. A missense mutation leading to p.G345V was found in family C of Ashkenazi Jewish origin and family E of Japanese origin. Two other missense mutations leading to p.V338E and p.T377M were identified in 2 other Japanese families. All of the amino acids involved are evolutionarily conserved in all vertebrates. The mutations were not observed in the Exome Variant Server, 10 Chinese and 32 French non-SCA subjects, or 1,248 chromosomes of French, Chinese, or Japanese controls. Our findings provide strong genetic support for *KCND3* being the causative gene in SCA19/22.

Kv4.3 is highly expressed in the brain, in particular in the cerebellar Purkinje cells, granule cells, basket cells, stellate cells, a subset of γ-aminobutyric acidergic deep neurons, and Lugaro cells adjacent to the somata of Purkinje cells.[19–23] Kv4.3 may play an important role in the development of cerebellum.[23,24] Of note, Kv4.3 is also expressed in the heart, and rare missense mutations in the cytoplasmic C-terminus have been implicated in Brugada syndrome,[25] which is a hereditary condition with cardiac arrhythmia predisposed to sudden cardiac death. There was no mention of neurological disorders in these patients. None of the patients in this report had cardiac symptoms or signs.

KCND3 encodes Kv4.3, an alpha subunit of the *Shal* family of the A-type voltage-gated K^+ channels which are important in membrane repolarization[19] in excitable cells. Similar to other voltage-gated K^+ channels, Kv4.3 forms homo- or heterotetramers with members of the *Shal* subfamily channels. Each alpha subunit has 6 transmembrane segments (S1–S6) and a re-entrant loop linking S5 and S6 (see Fig 2D). S1 through S4 form the voltage sensing domain, whereas S5, S6, and the re-entrant loop form the ion selective pore. F227 resides in S2 and is conserved between Kv4 and Kv1 of the *Shaker* family, which, similar to *Shal*, also carries a voltage-dependent potassium current. F227 is equivalent to F223 in Kv1.2 and F280 in *Shaker*. Functionally, F227 has been suggested to be a high-impact residue that indirectly coordinates the omega pathway, which is formed by S1–S3 helices and S4 movement in response to membrane voltage changes.[26,27] Thus, p.F227del may lead to a shift in the downstream residues in S2 lining the ion permeation pathway to interfere with the normal movement

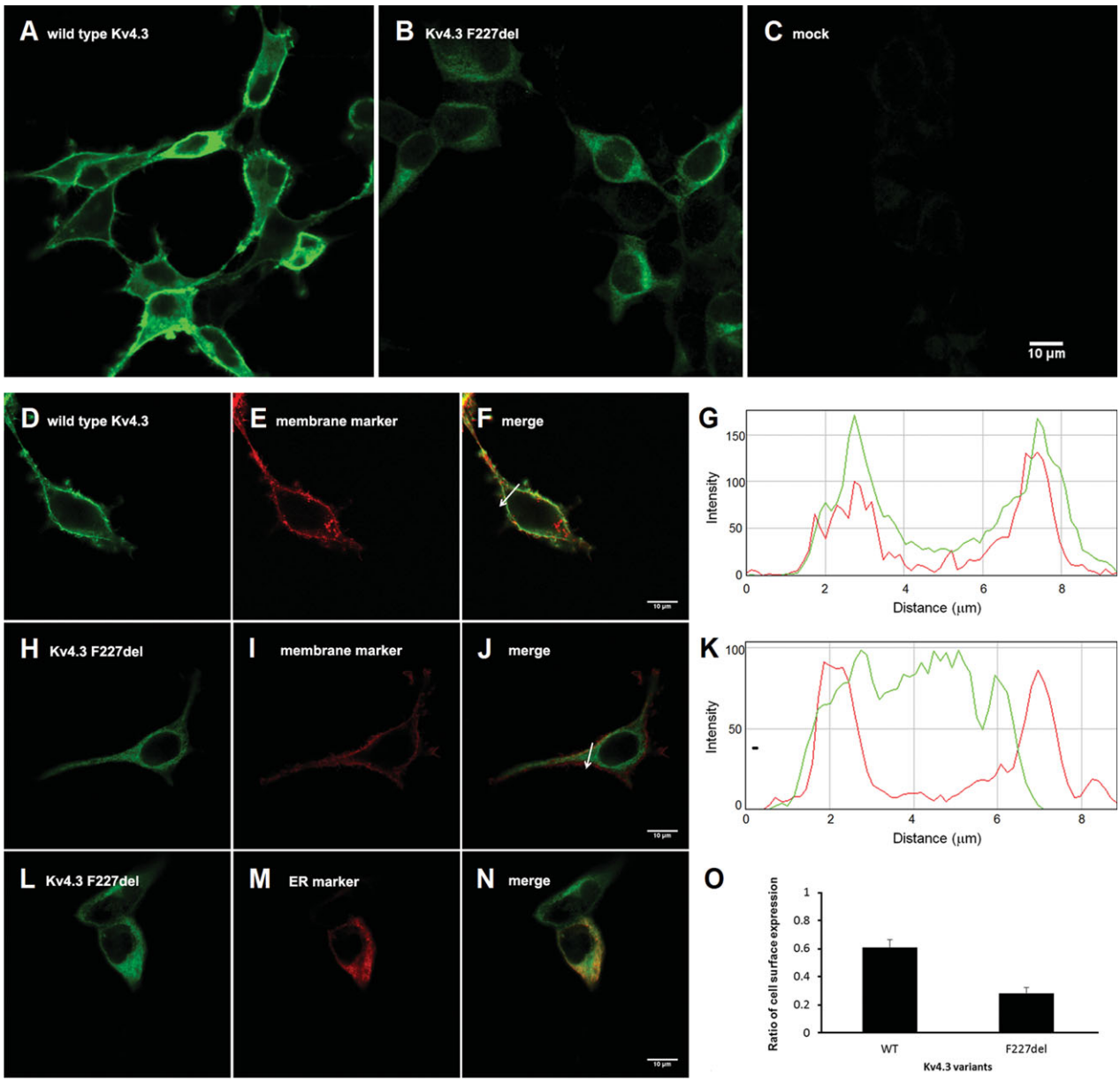

FIGURE 3: Confocal images demonstrating impaired cell surface expression and cytoplasmic retention of the mutant F227del Kv4.3. HEK-293T cells were transiently transfected with wild-type (WT; A) or p.F227del mutant (B) human Kv4.3, or empty vector (C) and immunostained with Kv4.3-specific antibody and green fluorophore-labeled secondary antibodies. Green fluorophore-labeled WT Kv4.3 (D) was expressed in the plasma membrane (E), colocalizing with DsRed-labeled membrane protein P0 (F). The spatial profile of fluorescent intensity of WT Kv4.3 (green) and P0 (red) along the arrow imposed on the images is shown in (G). The x-axis displays the distance relative to the start point of the arrow, and the y-axis displays the fluorescence intensity. F227del Kv4.3 (H) was deficient in targeting to the plasma membrane (I, J). The spatial profile of fluorescent intensity of F227del Kv4.3 (green) and P0 (red) along the arrow imposed on the images is shown in (K). Instead, F227del Kv4.3 was retained in the cytoplasm (L) and colocalized with an endoplasmic reticulum-specific marker (M, N). The ratio of cell surface expression for the p.F227del Kv4.3 was significantly lower (O) than that observed in the WT Kv4.3 (mean ± standard error of the mean, p.F227del: 0.28 ± 0.04, n = 10; WT Kv4.3: 0.61 ± 0.06, n = 10; $p = 0.0014$, paired *t* test). Scale bar = 10µm.

of S4. Empirically, we were surprised not to be able to detect any channel activity or changes in the biophysical properties of the channel (see Fig 4). Instead, we observed intracellular retention, suggesting that p.F227del causes a loss of channel function by interfering with proper plasma membrane targeting and incorporation into a functional tetrameric channel complex (see Fig 3).

V338 resides in S5, and both G345 and T377 are in the putative outer vestibule of the channel between transmembrane segments S5 and S6. Efforts are underway to continue to characterize the functional consequences of mutations in *KCND3*.

Following *KCNA1* (Kv1.1, NM_000217) and *KCNC3* (Kv3.3, NM_004977), *KCND3* (Kv4.3,

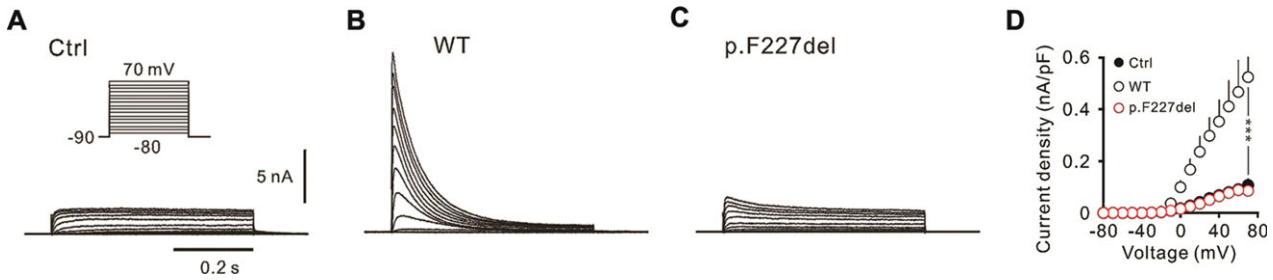

FIGURE 4: Electrophysiological recordings of the Kv4.3 channels. Whole cell patch-clamp recordings revealed endogenous currents in untransfected cells (A), large rapidly inactivating A-type potassium current in wild-type (WT) Kv4.3-transfected cells (B), and reduced current amplitudes in p.F227del Kv4.3-transfected cells (C). WT *(open black circles)* had a significantly larger current density than p.F227del (*red circles;* ***$p < 0.0005$), and the current density of p.F227del was similar to that of controls (Ctrl; *filled black circles;* D).

NM_004980) is the third voltage-gated potassium channel gene discovered to cause human cerebellar ataxia. Point mutations[28–33] in *Shaker* Kv1.1-encoding *KCNA1* cause episodic ataxia type 1 (OMIM160120). Point mutations in *Shaw*-related Kv3.3-encoding *KCNC3* cause SCA13 (OMIM605259), with phenotypes ranging from neurodevelopmental disorders to adult onset neurodegeneration.[34,35] Although the exact mechanism is not yet known how mutations may disrupt Kv4.3 function in regulating neuronal excitability and how this may in turn lead to neurodegeneration, the discovery of *KCND3* as the causative gene in SCA19/22 adds to the growing evidence of the importance of fine tuning neuronal excitability in the health and survival of neurons and especially cerebellar neurons. Other voltage-gated K^+ channels have been proposed in neurodegenerative diseases.[36–38]

Patients with p.F227del in Kv4.3 all have a protracted clinical course, with slowly progressive cerebellar ataxia. As proposed, the phenotypes of dominant cerebellar ataxias due to mutations other than polyglutamine expansions are slow and less complicated despite earlier age at onset.[4] There are clinical differences between families A and B. The Chinese family presents with relatively pure cerebellar signs, which are consistent with the clinical classification of autosomal dominant cerebellar ataxia (ADCA) type III,[39] similar to SCA6, whereas the French family presents with signs consistent with ADCA type I.[39] The clinical progression of SCA22 appears even slower than that of SCA6, as evaluated with the clinical rating scale of ataxia SARA.[9] For individuals carrying the p.F227del mutation, the onset of ataxia was earlier (15–30 years) in the younger generation than in the older (30–50 years), which is also true for those with the p.G345V mutation, although the age at onset was later (50s in the older generation, compared to 30s–40s in the younger generation), suggesting that the G345V-associated phenotype may be milder. Of note, the disease is almost fully penetrant in the 6 families described in this report. It is our hope and expectation that additional patients and families will be identified with SCA19/22 to further define the clinical features.

Acknowledgment

This work was supported by funds from the Taiwan Ataxia Association; the Hsu Tsung Pei Medical Research Fund; and research grants from Taipei Veterans General Hospital (V99-C1-023, V99-C1-052, V100C-036, and V101C-045); the National Science Council, Taiwan, ROC (NSC95-2320-B-010-056-MY3, NSC96-2314-B-010-036-MY3, NSC98-2320-B-010-029-MY3, and NSC99-2314-B-010-013-MY3); the Ministry of Education, Aim for the Top University Plan (V100-E6-006 and V101E7-005), Taiwan; the European Union (6th Framework Program for Research and Development call, to the EUROSCA consortium); the VERUM Foundation (A.B.), the Association Connaitre les Syndromes Cérébelleux (to G.S. and to the SPATAX Network), and the NIH (grant 3R21DC010074; K.M., J.Z.L., and M.B.). The sequencing and analytical work was supported by the High-Throughput Genome Analysis Core Facility of the National Core Facility Program for Biotechnology, Taiwan (NSC-100-2319-B-010-001), National Core Facility Program for Biotechnology (Taiwan Bioinformatics Consortium of Taiwan, NSC-100-2319-B-010-002), and University of Michigan DNA Core. Fluorescence microimaging analysis (confocal microscopy or live cell microscopy) was performed by the Public Instrumental Service Center at the Department of Medical Research and Education, Taipei Veterans General Hospital, Taipei, Taiwan, R.O.C.

We thank all patients for participating in this study; Dr S. Forlani for DNA preparation; Drs M.-L. Tsaur, T.-S. Su, U.-C. Yang, and W.-C. Yu for constructive suggestions; J. Dell'Orco, L. Gates, and W. Peng for

assistance with specific experiments; and J. Xu for bioinformatics.

Authorship

Y.-C.Le., A.D., and K.M. contributed equally.

Potential Conflicts of Interest

A.D.: consultancy, Pfizer; grants/grants pending, Agence Nationale de la Recherche. A.B.: consultancy, Wolfson Foundation; grants/grants pending, Agence Nationale de la Recherche. M.B.: grants/grants pending, National Ataxia Foundation; travel expenses, Society for Biological Psychiatry 2011, Humboldt College 2012 Havana Cuba, CINP 2010 Hong Kong. G.S.: grants/grants pending, Agence Nationale de la Recherche; travel expenses, Roche.

References

1. Klockgether T. Update on degenerative ataxias. Curr Opin Neurol 2011;24:339–345.
2. Soong B- W, Paulson HL. Spinocerebellar ataxias: an update. Curr Opin Neurol 2007;20:438–446.
3. Soong BW, LU YC, Choo KB, Lee HY. Frequency analysis of autosomal dominant ataxias in Taiwanese patients and clinical and molecular characterization of spinocerebellar ataxia type 6. Arch Neurol 2001;58:1105–1109.
4. Durr A. Autosomal dominant cerebellar ataxias: polyglutamine expansions and beyond. Lancet Neurol 2010;9:885–894.
5. Chung MY, Lu YC, Cheng NC, Soong BW. A novel autosomal dominant spinocerebellar ataxia (SCA22) linked to chromosome 1p21-q23. Brain 2003;126:1293–1299.
6. Verbeek DS, Schelhaas JH, Ippel EF, et al. Identification of a novel SCA locus (SCA19) in a Dutch autosomal dominant cerebellar ataxia family on chromosome region 1p21-q21. Hum Genet 2002; 111:388–393.
7. Schelhaas HJ, Verbeek DS, Van de Warrenburg BP, Sinke RJ. SCA19 and SCA22: evidence for one locus with a worldwide distribution. Brain 2004;127:E6; author reply E7.
8. Schmitz-Hubsch T, du Montcel ST, Baliko L, et al. Scale for the assessment and rating of ataxia: development of a new clinical scale. Neurology 2006;66:1717–1720.
9. Lee YC, Liao YC, Wang PS, et al. Comparison of cerebellar ataxias: a three-year prospective longitudinal assessment. Mov Disord 2011;26:2081–2087.
10. Sambrook J, Russell DW. Molecular cloning: a laboratory manual. 3rd ed. Cold Spring Harbor, NY: Cold Spring Harbor Laboratory Press, 2001.
11. Abecasis GR, Cherny SS, Cookson WO, Cardon LR. Merlin—rapid analysis of dense genetic maps using sparse gene flow trees. Nat Genet 2002;30:97–101.
12. Purcell S, Neale B, Todd-Brown K, et al. PLINK: a tool set for whole-genome association and population-based linkage analyses. Am J Hum Genet 2007;81:559–575.
13. Durbin RM, Altshuler D, Abecasis GR, et al. A map of human genome variation from population-scale sequencing. Nature 2010; 467:1061–1073.
14. Postma AV, Bezzina CR, de Vries JF, et al. Genomic organisation and chromosomal localisation of two members of the KCND ion channel family, KCND2 and KCND3. Hum Genet 2000;106: 614–619.
15. Norris AJ, Nerbonne JM. Molecular dissection of I(A) in cortical pyramidal neurons reveals three distinct components encoded by Kv4.2, Kv4.3, and Kv1.4 alpha-subunits. J Neurosci 2010;30: 5092–5101.
16. Niwa N, Nerbonne JM. Molecular determinants of cardiac transient outward potassium current (I(to)) expression and regulation. J Mol Cell Cardiol 2010;48:12–25.
17. Lee YC, Yu CT, Lin KP, et al. MPZ mutation G123S characterization: evidence for a complex pathogenesis in CMT disease. Neurology 2008;70:273–277.
18. Shi G, Kleinklaus AK, Marrion NV, Trimmer JS. Properties of Kv2.1 K+ channels expressed in transfected mammalian cells. J Biol Chem 1994;269:23204–23211.
19. Tsaur ML, Chou CC, Shih YH, Wang HL. Cloning, expression and CNS distribution of Kv4.3, an A-type K+ channel alpha subunit. FEBS Lett 1997;400:215–220.
20. Kong W, Po S, Yamagishi T, et al. Isolation and characterization of the human gene encoding Ito: further diversity by alternative mRNA splicing. Am J Physiol 1998;275:H1963–H1970.
21. Dilks D, Ling HP, Cockett M, et al. Cloning and expression of the human kv4.3 potassium channel. J Neurophysiol 1999;81: 1974–1977.
22. Isbrandt D, Leicher T, Waldschutz R, et al. Gene structures and expression profiles of three human KCND (Kv4) potassium channels mediating A-type currents I(TO) and I(SA). Genomics 2000; 64:144–154.
23. Hsu YH, Huang HY, Tsaur ML. Contrasting expression of Kv4.3, an A-type K+ channel, in migrating Purkinje cells and other post-migratory cerebellar neurons. Eur J Neurosci 2003;18:601–612.
24. Oberdick J, Baader SL, Schilling K. From zebra stripes to postal zones: deciphering patterns of gene expression in the cerebellum. Trends Neurosci 1998;21:383–390.
25. Giudicessi JR, Ye D, Tester DJ, et al. Transient outward current (I(to)) gain-of-function mutations in the KCND3-encoded Kv4.3 potassium channel and Brugada syndrome. Heart Rhythm 2011;8: 1024–1032.
26. Tombola F, Pathak MM, Gorostiza P, Isacoff EY. The twisted ion-permeation pathway of a resting voltage-sensing domain. Nature 2007;445:546–549.
27. Khalili-Araghi F, Tajkhorshid E, Roux B, Schulten K. Molecular dynamics investigation of the omega-current in the Kv1.2 voltage sensor domains. Biophys J 2012;102:258–267.
28. D'Adamo MC, Liu Z, Adelman JP, et al. Episodic ataxia type-1 mutations in the hKv1.1 cytoplasmic pore region alter the gating properties of the channel. EMBO J 1998;17:1200–1207.
29. D'Adamo MC, Imbrici P, Sponcichetti F, Pessia M. Mutations in the KCNA1 gene associated with episodic ataxia type-1 syndrome impair heteromeric voltage-gated K(+) channel function. FASEB J 1999;13:1335–1345.
30. Eunson LH, Rea R, Zuberi SM, et al. Clinical, genetic, and expression studies of mutations in the potassium channel gene KCNA1 reveal new phenotypic variability. Ann Neurol 2000;48:647–656.
31. Rea R, Spauschus A, Eunson LH, et al. Variable K(+) channel subunit dysfunction in inherited mutations of KCNA1. J Physiol 2002; 538:5–23.
32. Imbrici P, D'Adamo MC, Kullmann DM, Pessia M. Episodic ataxia type 1 mutations in the KCNA1 gene impair the fast inactivation properties of the human potassium channels Kv1.4-1.1/Kvbeta1.1 and Kv1.4-1.1/Kvbeta1.2. Eur J Neurosci 2006;24:3073–3083.
33. Shook SJ, Mamsa H, Jen JC, et al. Novel mutation in KCNA1 causes episodic ataxia with paroxysmal dyspnea. Muscle Nerve 2008;37:399–402.

34. Waters MF, Minassian NA, Stevanin G, et al. Mutations in voltage-gated potassium channel KCNC3 cause degenerative and developmental central nervous system phenotypes. Nat Genet 2006;38:447–451.

35. Figueroa KP, Waters MF, Garibyan V, et al. Frequency of KCNC3 DNA variants as causes of spinocerebellar ataxia 13 (SCA13). PLoS One 2011;6:e17811.

36. Ariano MA, Cepeda C, Calvert CR, et al. Striatal potassium channel dysfunction in Huntington's disease transgenic mice. J Neurophysiol 2005;93:2565–2574.

37. Angulo E, Noe V, Casado V, et al. Up-regulation of the Kv3.4 potassium channel subunit in early stages of Alzheimer's disease. J Neurochem 2004;91:547–557.

38. Baranauskas G, Tkatch T, Surmeier DJ. Delayed rectifier currents in rat globus pallidus neurons are attributable to Kv2.1 and Kv3.1/3.2 K(+) channels. J Neurosci 1999;19:6394–6404.

39. Harding AE. Clinical features and classification of inherited ataxias. Adv Neurol 1993;61:1–14.